

Biometric System using Iris Pattern Recognition

Samarth S. Mabrukar, Nitin S. Sonawane, Jasmine A. Bagban

Abstract—Iris is unique body part which does not change with respect to time. Also every individual has unique and different pattern of the Iris for both the eyes. This helps in identifying a person, quite accurately. Initially, a filter must be employed to get rid of any kind of noises before pre-processing stage. Initially we detect the pupil-iris boundary. After that, we give it to Circular Hough transform to detect its center which will be used to extract iris from the image. Using Daugman’s Rubber sheet model, we normalize the iris pattern for making computations easy. Feature Extraction is done by using multi-scale Taylor series expansion of the iris texture. Feature vectors are extracted by binarizing the first and second order multi-scale Taylor coefficients. The proposed algorithm is tested against different images which gives better results in less computation time. The simulation is carried out using CASIA database on MATLAB.

Index Terms—Hough Transform, Iris, Multi-Scale, Segmentation, Taylor Series Expansion.

I. INTRODUCTION

Identification of a person to be himself has always been an important and difficult task. People, today, are being identified by their Signatures, PIN codes or passwords. But in today’s digital era, it is quite easy to forge the identification by stealing their PIN or passwords. Hence, what is required is an identification system based on attributes of a person which is impossible to steal. The Iris, with its unique features, will provide a solution to this problem.

Iris patterns are formed by combined layers of pigmented epithelial cells, muscles for controlling the pupil, a stromal layer consisting of connective tissue, blood vessels and an anterior border layer [1]. These Iris patterns are random in nature, which make them statistically unique and suitable for biometric measurements [2]. The Iris Pattern is so unique that, no two persons can have the same Iris structure, not even the same person’s two eyes have the same structure of iris. As an internal organ, iris is well protected from the external environment.

An iris recognition system consists of four main stages: (i) image acquisition, (ii) Pre-processing, which includes iris localization, image normalization and polar transformation, (iii) Iris feature Extraction and (iv) Iris template matching. In feature extraction, we are using Multi-scale Taylor series Expansion as it helps in reducing the size of the iris template

which is vital for efficient processing in large-scale applications [8]. In our system, we are using the iris images form CASIA database [3]. Hence we do not need to perform the first step, i.e. image acquisition. We directly start from the pre-processing stage.

II. IRIS PRE-PROCESSING

The first stage of pre-processing consists of localizing the iris in an iris image. The acquired iris image has to be pre-processed to detect the iris, which is an annular portion between the pupil (inner boundary) and the sclera (outer boundary). The iris images present in CASIA database are greyscale images. Hence, the effects of illumination are not present. The first step in iris localization is to detect pupil which is the black circular part surrounded by iris tissues. The center of pupil can be used to detect the outer radius of iris patterns. The important steps involved are:

A. Pupil Detection (Inner Iris Localization)

To find the pupil in the iris, the first thing to do is to find the edge between the pupil and iris. As there is high contrast between the pupil and iris, it is not difficult to detect this edge.

In this, we are using logical edge detection. For this, we have observed Canny operator as given in [4] and [12]. By observing that, we conclude that Gaussian smoothing suppresses many important edges. Therefore we neglect this part. In this algorithm, we are using following steps:

1. Use improved Sobel operator [11]. The main reason for using this operator is that it returns high gradient value for any change in the grey-level.

$$T_x = \begin{bmatrix} 2 & 3 & 0 & -3 & -2 \\ 3 & 4 & 0 & -4 & -3 \\ 6 & 6 & 0 & -6 & -6 \\ 3 & 4 & 0 & -4 & -3 \\ 2 & 3 & 0 & -3 & -2 \end{bmatrix}$$

$$T_y = \begin{bmatrix} 2 & 3 & 6 & 3 & 2 \\ 3 & 4 & 6 & 4 & 3 \\ 0 & 0 & 0 & 0 & 0 \\ -3 & -4 & -6 & -4 & -3 \\ -2 & -3 & -6 & -3 & -2 \end{bmatrix}$$

2. After applying these two masks we take the gradient of the convolved images as:

$$G(X, Y) = \sqrt{G_x(X, Y)^2 + G_y(X, Y)^2}$$

3. After this we shall find their angles as:

$$\theta = \tan^{-1} \frac{G_x(X, Y)}{G_y(X, Y)}$$

4. Now we shall perform grey level slicing i.e. taking selected no of values suppressing the weak edges and retaining strong edges within threshold T_1 and T_2 ($T_2 > T_1$).
5. Track the desired region or portion i.e. the circular pupil-iris boundary.

Manuscript published on 30 April 2013.

*Correspondence Author(s)

Samarth S. Mabrukar, Department of Electronics and Telecommunication, Sinhgad Academy of Engineering, Pune, India.

Nitin S. Sonawane, Department of Electronics and Telecommunication, Sinhgad Academy of Engineering, Pune, India.

Jasmine A. Bagban, Department of Electronics and Telecommunication, Sinhgad Academy of Engineering, Pune, India.

© The Authors. Published by Blue Eyes Intelligence Engineering and Sciences Publication (BEIESP). This is an open access article under the CC-BY-NC-ND license <http://creativecommons.org/licenses/by-nc-nd/4.0/>.

6. Now we shall perform Non-maxima suppression as given in [12] by the references of “ θ ”.

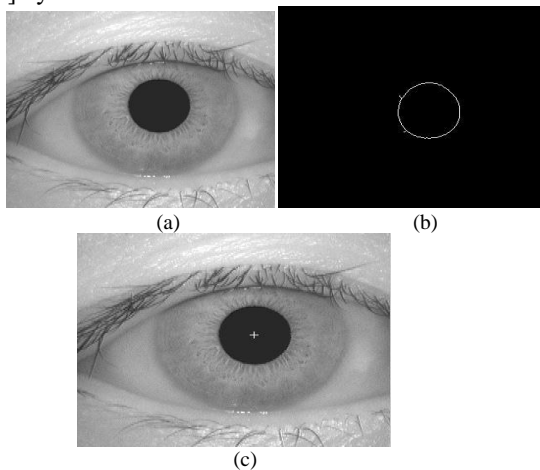


Fig. 1 Steps involved in detection of inner pupil boundary:

a)Test Image b)Proposed Edge Image c)Center of Pupil marked by ‘+’.

7. After performing the above operations we get all the important edges.
8. We use the concept of 8-connectivity to select all strong edges.
9. Apply morphology to thin the edges as much as possible.

The next step is to find the pupil center and pupil radius. For this, we use Circular Hough Transform [5]. The basic idea of this technique is to find curves that can be parameterized like straight lines, polynomials, circles, etc., in a suitable parameter space. The transformation is able to overcome irregularities and noise. The Binary image after Logical Edge detection is given as input to Hough Transform for further processing. Circular Hough transform gives the center and radius of the edge between pupil and radius, which is basically a circle.

A circle basically has two parameters: center and radius. The edge pixels in the binary image are bright. From this edge map, votes are cast in Hough space or accumulator space for the center coordinates (x_c, y_c) , and the radius r of circles passing through each edge point. In our case, we give the approximate radius of pupil as input and check the number of votes cast for the approximate center, in the Hough space. This process is repeated for a range of radii, until we get the max votes at some point, which gives the pupil center and radius.

B. Outer Iris Localization

Pupil and Iris center in our database images are almost coincident. Hence there is no need to repeat the above procedure for Iris center. To find the iris radius, we find the first derivative of the circular summation.

To find the iris radius, we take the sum of all the pixels lying on the circumference, for a range of radius from the center which is obtained from Hough transform. This value (sum) is then stored and this procedure is repeated for the next value of radius. Then we find the difference in the two values. This gives the first derivative of the circular summation. This procedure is repeated until we get the maximum first derivative. This maximum value corresponds to the outer iris edge.

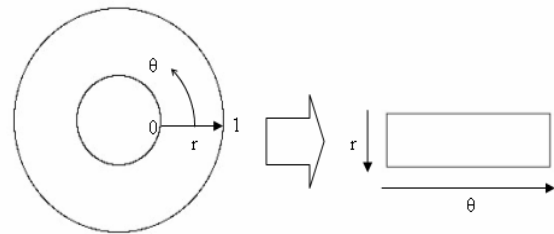


Fig. 2 Daugman's Rubber Sheet model

The value of radius for which we get this maximum value, is the outer iris radius. We have found iris center, pupil radius and outer iris radius. Hence the localization part is complete.

C. Iris Normalization

After iris localization, we have to normalize it in order to enable the generation of the feature vector and their comparisons. There are many variations in the image of the eye, like optical size of the iris, position of pupil in the iris, varying imaging distance, rotation of the camera, head tilt and rotation of the eye within the eye socket. Also the iris orientation changes from person to person. Hence it is required to normalize the iris image so that the representation is common to all, with similar dimensions. Therefore, this normalization process will produce irises with same fixed dimensions so that two photographs for the same iris under different lighting conditions will have the same characteristic features.

The concept of rubber sheet modal suggested by Daugman [6] takes into consideration the possibility of pupil dilation and appearing of different size in different images. For this purpose, the coordinate system is changed by unwrapping the iris and mapping all the points within the boundary of the iris into their polar equivalent as shown in Figure 2.

This model remaps each point within the iris region to a pair of polar coordinates (r, θ) where r is on the interval $[0, 1]$ and θ is angle $[0, 2\pi]$. Thus the following set of equations are used to transform the annular region of iris into polar equivalent.

$$I(x(\rho, \theta), y(\rho, \theta)) \rightarrow I(\rho, \theta)$$

with

$$x_p(\rho, \theta) = x_{p0}(\theta) + r_p * \cos(\theta)$$

$$y_p(\rho, \theta) = y_{p0}(\theta) + r_p * \sin(\theta)$$

$$x_i(\rho, \theta) = x_{i0}(\theta) + r_i * \cos(\theta)$$

$$y_i(\rho, \theta) = x_{i0}(\theta) + r_i * \sin(\theta)$$

Where, r_p and r_i are the radii of pupil and the iris respectively, while $(x_p(\theta), y_p(\theta))$ and $(x_i(\theta), y_i(\theta))$ are the coordinates of the pupil and iris boundaries in the direction θ . The value of θ belongs to $[0, 2\pi]$, ρ belongs to $[0, 1]$.

Using Daugman's rubber sheet model for normalizing the iris region, the pupil center is considered as the Reference point, and radial vectors pass through the iris region. The radial resolution is represented by a number of data points that are selected along each radial line. The angular resolution is defined as the number of radial lines going around the iris region. From the 'doughnut' iris region, normalization produces 2D array with horizontal dimensions of angular resolution and vertical dimensions of radial resolution. Another 2D array was created for marking reflections, eyelashes, and eyelids detected in the segmentation stage.

In order to prevent non-iris region data from corrupting normalized representation, data points which occur along the pupil border or the iris border are discarded.

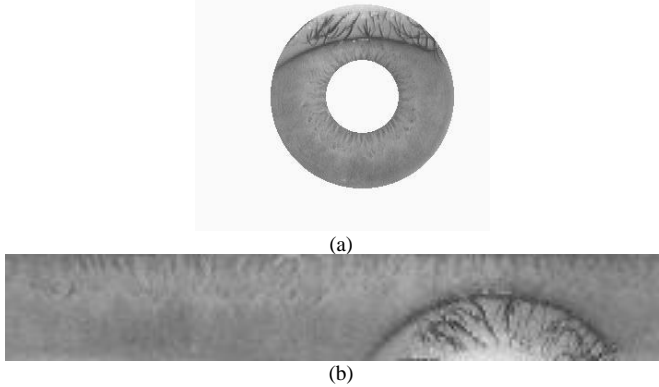


Fig. 3 Iris Normalization (a)Polar arrangement of Iris,(b) Normalized arrangement of Iris.

As in Daugman’s rubber sheet model, removing rotational inconsistencies is performed at the matching stage.

Therefore, if the pupil dilates, the same points are picked up and mapped again which makes the mapping process stretch invariant [7]. After some experimentation [8], it was found that an iris template size of 256×32 gives the best compromise between speed and accuracy for the iris template matching.

III. FEATURE EXTRACTION

For the correct identification of individuals, the most discriminating features present in the iris pattern, must be extracted. Only the significant features of the iris must be encoded so that comparisons between templates can be made. The iris has an interesting structure and presents plentiful texture information. To store such a lot of spatial detail, it is helpful to make use of a multiscale representation. Our method uses phase based features from the multi-scale Taylor expansion [8]. Using Phase-based iris recognition algorithms improves speed of operation and also increases verification performance [9]. The iris recognition system employed by us, extracts features from binarized multi-scale Taylor expansion phase information. For the binary feature vector, code ‘0’ corresponds to a negative sign of the expansion and similarly, code ‘1’ corresponds to positive sign of the expansion. As Multi-scale Taylor expansion can be computed efficiently and has a transparent interpretation, this method was chosen. The features extracted Taylor’s coefficients have a greater localization in the spatial domain. Because of this, feature resolution in the frequency domain reduces. This relation of localization in space and frequency domains is natural for the iris where local objects as freckles, furrows, stripes, coronas dominate the texture, and where periodic texture patterns that are well localized in frequency domain are rare [8].

Consider the iris pattern at a specific pseudo-polar radius, ‘ $r = \text{const}$ ’ as an analytic one-dimensional signal $u = u(x)$, where x denotes the pseudo-polar angle. We can represent any analytic signal as a classic Taylor series expansion centered on any fixed point $x = x_i$. The 0^{th} coefficient of the expansion, $u(x_i)$ basically gives the pixel intensity value at that point. We know that the intensity value is strongly influenced by iris illumination conditions; hence the 0^{th} coefficient is neglected. The first and second order coefficients are given as $u'(x_i) / 1!$ and $u''(x_i) / 2!$. The first derivative $u'(x)$ measures the rate of change in the pixel value, of the signal around point x , i.e. if $u'(x) > 0$, then $u(x)$ is increasing around point x and if $u'(x) < 0$ then $u(x)$ is decreasing around the same point. The sign of

the second derivative $u''(x)$ gives the type of concavity of a graph $\{x, u(x)\}$ around x , i.e. if $u''(x) > 0$ then $\{x, u(x)\}$ is concave upward and if $u''(x) < 0$ then the graph $\{x, u(x)\}$ is concave downward around point x [8].

The first and the second terms of the Taylor series expansion define the linear and the quadratic behavior of $u(x)$ around x , respectively. The extreme points of the first derivative indicate points where the signal u has its greatest local asymmetry and the extreme points of second derivative indicate points of great local symmetry of $u(x)$. We can also say that the real part of the familiar Gabor response at a point x is similar to the second order Taylor coefficient centered at the point x and imaginary part the Gabor response is alike to the first order Taylor coefficient [8]

A. Binary features as local iris features

Previously we defined the binary feature vectors using Taylor series expansion. Here we define the iris eight binary features simply by binarizing the blurred first and second order Taylor coefficients $u_x, u_{xx}, u_y,$ and u_{yy} . Suppose we blur with scales σ_x and σ_y , and we have $u_x(i, j) > 0$ at a point (i, j) belonging to the iris region bounded by the two convex iris contours, then we set the binary feature $(u_x)_{ij} = 1$. Similarly, if $u_x(i, j) < 0$, then the binary feature is set to $(u_x)_{ij} = 0$. Finally, if the point (i, j) does not belong to the iris region bounded by two convex contours or if $u_x(i, j) = 0$, then the binary feature $(u_x)_{ij}$ is chosen randomly with equal probability. As opposed to the binary features that are used to describe the phase of Gabor responses, the binary features that we get, has a transparent interpretation. If u_x has the value $(u_x)_{ij} = 1$ when blurred at scales σ_x and σ_y it means that the iris texture at scale σ_x and σ_y increases along angular direction around (i, j) point. If, on the other hand, $(u_{yy})_{ij} = 0$, one can state that the iris texture is concave along radial direction around (i, j) point [8].

Since we use eight different continuous two dimensional multiscale Taylor expansion coefficients, we obtain eight binary maps after binarization. At any fixed location (i, j) , we can form an eight bit number using the eight bits of binary features. Hence we form a byte type feature.

$$\sum_{k=0}^7 f[i][j]$$

where, $f[i][j] = \{\text{feature bit of } k^{\text{th}} \text{ binary map at position } (i, j)\} 2^k$, i and j gives the angular and radial positions in the unwrapped iris image.

IV. MATCHING

A matching technique is required to match the template that is generated in the feature encoding process, which gives a measure of similarity between two iris templates. This metric should give one range of values when comparing templates generated from the same eye, known as intra-class comparisons, and another range of values when comparing templates created from different irises, known as inter-class comparisons. These two cases should give distinct and separate values, so that a decision can be made with high confidence as to whether two templates are from the same iris, or from two different irises [10].

The conventional approach, given by Daugman uses Hamming distance for matching two binary iris templates. Hamming Distance is calculated for different angular shifts and the final distance is the minimum of all calculated distances. To be more consistent with our feature extraction method, we will construct a similarity measure instead of a distance measure. A similarity measure of a pair of iris images is given by the maximal number of matched bits of their binary features maps where the maximization is performed over a fixed number of angular shifts. However, such a similarity measure underestimates the similarity of genuine pairs that have slight segmentation inaccuracies [8]. Hence, in our iris recognition system, the method used for iris template matching is the Elastic similarity metric for comparison of binary feature maps [8].

V. CONCLUSIONS

In this paper, we propose and evaluate a scheme for accurately localizing the iris in images acquired for iris recognition systems. Daugman's Rubber Sheet Model was also successfully implemented. In our experiments, multi-scale Taylor-based features are pretty much immune to illumination changes. This is partially due to neglecting the 0th Taylor coefficient. Feature extraction using Multi-scale Taylor expansion was also implemented and it yielded good results.

REFERENCES

1. F.H. Adler, Physiology of the Eye, Mosby, St. Louis, MO, 1965.
2. J. Daugman, High confidence visual recognition of persons by a test of statistical independence, IEEE Transactions on Pattern Analysis and Machine Intelligence 15 (11) (1993) 1148–1161.
3. Chinese Academy of Sciences – Institute of Automation Iris Database 1.0, 2003. Available at: <<http://www.sinobiometrics.com>>.
4. J. Canny (1986) "A computational approach to edge detection", IEEE Trans. Pattern Analysis and Machine Intelligence, vol 8, pages 679-714.
5. T. Chuan Chen, K. Liang Chung: An Efficient Randomized Algorithm for Detecting Circles. Computer Vision and Image Understanding Vol. 83 (2001) 172-191.
6. J. Daugman. How Iris Recognition Works. Proceedings of 2002 International Conference on Image Processing, Vol. 1, 2002. Available at http://www.ncits.org/tc_home/m1htm/docs/m1020044.pdf
7. Y. Zhu, T. Tan, Y. Wang: Biometric Personal Identification Based on Iris Patterns. Proceedings of ICPR, International Conference on Pattern Recognition Vol. II (2000) 805-808.
8. Algirdas Bastys, Justas Kranauskas, Volker Krüger, "Iris recognition by fusing different representations of multi-scale Taylor expansion", Science Direct journals, Computer Vision and Image Understanding 115 (2011) 804–816.
9. J. Daugman, New methods in iris recognition, IEEE Transactions on Systems, Man, and Cybernetics – Part B: Cybernetics 37 (5) (2007) 1167–1175.
10. Masek, L. (2003). Recognition of Human Iris Patterns for Biometric Identification. Available at: <<http://www.csse.uwa.edu.au/opk/studentprojects/labor>>.
11. Zhang Jin-Yu, Chen Yan, Huang Xian-Xiang, Edge Detection of Images Based on Improved Sobel Operator and Genetic Algorithms.
12. R.C.Gonzalez and R.Woods," Digital Image Processing, 3rd edition", Pearson Publication, Pg 741.